General Disclaimer

One or more of the Following Statements may affect this Document

- This document has been reproduced from the best copy furnished by the organizational source. It is being released in the interest of making available as much information as possible.

- This document may contain data, which exceeds the sheet parameters. It was furnished in this condition by the organizational source and is the best copy available.

- This document may contain tone-on-tone or color graphs, charts and/or pictures, which have been reproduced in black and white.

- This document is paginated as submitted by the original source.

- Portions of this document are not fully legible due to the historical nature of some of the material. However, it is the best reproduction available from the original submission.

NSG-2112

TRANSONIC FLUID DYNAMICS

Report TFD 78-04

H. Sobieczky, K-Y. Fung, A. R. Seebass, N. J. Yu

A NEW METHOD FOR DESIGNING SHOCK-FREE TRANSONIC CONFIGURATIONS

July 1978

ENGINEERING EXPERIMENT STATION
COLLEGE OF ENGINEERING
THE UNIVERSITY OF ARIZONA
TUCSON, ARIZONA

H. Sobieczky, K-Y. Fung, A. R. Seebass, N. J. Yu

A NEW METHOD FOR DESIGNING SHOCK-FREE TRANSONIC CONFIGURATIONS

Presented at the

AIAA 11th FLUID
AND PLASMA DYNAMICS
CONFERENCE

Seattle, Wash./July 10-12, 1978

Paper 78-114

A NEW METHOD FOR DESIGNING SHOCK-FREE TRANSONIC CONFIGURATIONS

H. Sobieczky*, N. J. Yu**, K-Y. Fung†, and A. R. Seebass††

University of Arizona
Tucson, Arizona 85721

Abstract

A new method for the design of shock-free supercritical airfoils, wings, and three-dimensional configurations is described. Results illustrating this procedure in two and three dimensions are given. They include modifications to part of the upper surface of an NACA 64A410 airfoil that will maintain shock-free flow over a range of Mach numbers for a fixed lift coefficient, and the modifications required on part of the upper surface of a swept wing with an NACA 64A410 root section to achieve shock-free flow. While the results are given for inviscid flow, the same procedures can be employed iteratively with a boundary layer calculation in order to achieve shock-free viscous designs. With a shock-free pressure field the boundary layer calculation will be reliable and not complicated by the difficulties of shock-wave boundary-layer interaction.

---

*Visiting Professor; Research Scientist, DFVLR, Göttingen, Germany. Member, AIAA.

**Senior Research Associate; now Research Scientist, the Boeing Commercial Airplane Company, Seattle, Washington. Member AIAA.

†Senior Research Associate. Member AIAA.

††Professor, Aerospace and Mechanical Engineering and Mathematics. Associate Fellow AIAA.

INTRODUCTION

Well-known requirements for increased efficiency, and in the case of aircraft, productivity, have forced the operating conditions of compressors, turbines, propellers, wing sections, and aircraft into the transonic regime. Unfortunately, once local regions of supersonic flow occur, shock waves are likely with the attendant wave drag, and boundary layer separation, losses. In the mid-fifties, Morawetz[1] proved that shock-free, two-dimensional, irrotational, near sonic flows are mathematically isolated. In other words, any small changes in the flow or boundary conditions that provide a shock-free flow will lead to the formation of a shock wave. Thus Morawetz's theorem stated that the shock-free inviscid flow solutions, if and when they existed, were isolated by neighboring solutions that contain shock waves. Recently this result has been extended to three dimensions by Cook.[2] Fortunately, it was recognized that such flows would have practical significance if, as seemed likaly, the shock waves that occurred in neighboring flows were very weak. Wind tunnel research by R. T. Whitcomb[3] at the NASA Langley Research Center and by H. H. Pearcey[4] at the National Physical Laboratory (U.K.) led to the development of practical "shock-free" airfoil sections. Subsequent analytical studies by Garabedian and Korn,[5] Nieuwland,[6] Boerstoel,[7] and Sobieczky[8] established theoretical design procedures for two-dimensional inviscid flows. More recently, the development of sophisticated numerical codes for the analysis of transonic flow fields has led to the design of both airfoils and wings by numerical optimization.[9,10] The practical success of the above efforts, as documented by the recent NASA Conference on Advanced Technology Research,[11] has been substantial. Further progress, as reported here, seems likely. The senior author recognized that the procedure he was using in the hodograph plane

implied an analogous procedure in the physical plane, and further, that this procedure did not seem to be restricted to two-dimensional flows.[12,13] This paper reports the success we have had to date in using this idea to provide shock-free designs in two and three dimensions.

The design procedure invoked here is, in principle, a simple one. While there is no guarantee that a shock-free flow will necessarily result from the procedure, our experience in two-dimensions has been that if the hodograph method will work for specified flow and airfoil parameters, then the procedure outlined here will work, too. Also, it provides neighboring shock-free airfoil shapes for fixed lift coefficient with varying Mach numbers and varying lift coefficient for fixed Mach numbers, as well as providing a multiplicity of closely related shapes that are shock-free at fixed lift coefficient and Mach number. This wealth of shock-free two-dimensional designs is of no great surprise; it is, then, not surprising that they are found with minimal computational effort. Two-dimensional inviscid flow potential airfoil designs require less than a minute of CYBER 175 CPU time and only a few seconds of CDC 7600 CPU time.

For three-dimensional flows our results are less extensive. Also, while it is clear that the procedure we use rests on a sound mathematical foundation in two dimensions, this may not be the case in three dimensions. Indeed, for three-dimensional (that is non-planar and non-axisymmetric) flows we are probably solving an ill-posed boundary value problem. The fact that shock-free flows are obtained in the cases studied here are a consequence of the pseudo-analytic character of the initial data and the particular numerical technique used to calculate the flow in the hyperbolic region.*

---

*The authors are indebted to Professor A. Jameson of the Courant Institute for alerting them to this difficulty.

We have demonstrated the ability to modify three-dimensional wings so that, within the context of the numerical algorithm used, shock-free flows are obtained. We have not yet demonstrated an analogous wealth of shock-free flows in the three-dimensional case, but see no reason to believe that this situation is different there. The practical consequences of this wealth should prove to be of interest to the aircraft industry.[14]

DESIGN PROCEDURE

The procedure we use to find shock-free designs assumes that a reliable numerical code is available for computing the flow past a given configuration, such as that sketched in Figure 1. Such codes are available for two- and three-dimensional inviscid flows. When they are coupled with a reliable boundary layer code, the design procedure outlined here can be used to calculate shock-free viscous flow designs. While this would require some modest iteration, it is certainly possible, both in practice and in principle. With the existence of a reliable analysis algorithm presumed, we modify this algorithm so that once the flow becomes hyperbolic we alter the basic equations so that they revert to elliptic behavior. This may be done in a number of ways, but it should be done in a way that it conserves new, but fictitious, "mass" and "momentum" fluxes to a satisfactory degree of accuracy. We may, for example, change the density's dependence from the usual one to one that returns the equations to elliptic form. We might suppose, for the purpose of illustration, that once the equations become parabolic, i.e., sonic, on some surface then at higher velocities the density will be maintained at its sonic value, giving elliptic equations. We use a numerical algorithm to compute this fictitious flow past a configuration of interest, chosen perhaps on the basis of previous design

experience. Because the equations are elliptic this will result in a discretized, pseudo-analytic, description of the velocity, density, and pressure fields on the embedded parabolic surfaces, and this description will be consistent with the correct governing equations. This initial data on the parabolic surfaces is then used to calculate the correct flow field inside such surfaces. This new flow field may, or may not, contain shock waves. This depends on the choice of the fictitious equations, or perhaps better, fictitious gas, used inside the parabolic surfaces. This new flow will define a stream surface that is tangent to, and has the same curvature as, the stream surface at the intersection of the sonic surface and the original body. Inside this surface a new body shape is defined by the stream surface of the new, but now real, flow.

Here, of course, we must also address the question of whether or not this initial value problem is well posed. In two dimensions there is no difficulty because either of the spatial coordinates may be designated as the time-like variable. This is not the case in three dimensions where only the spatial coordinate aligned with the flow is time-like. Because shock-free flows are reversible, the domains of dependence and influence may be interchanged. But neither the normal (nor the binormal) to the stream direction can be considered time-like in the three-dimensional initial value problem. Thus, it may be ill-posed because data are given on surfaces that are not in the usual domain of dependence. If so, any computational algorithm will be unstable for the three-dimensional problem. Further, while such computations can be stabilized by artificial means, the results must be considered suspect until they are verified by an independent computation. It is this fact that has made us stress that a reliable analysis algorithm should be the basis for the design computations. For

two-dimensional (planar and axisymmetric) designs this difficulty does not occur because the lateral coordinate can be considered to be the time-like direction. A simplistic analysis of model problems indicates that variations in the spanwise direction that are on a scale that is small compared to the nominal axial (flow direction) distance may amplify; thus the success of the numerical algorithm here may depend upon its natural filtering of such disturbances. This is not the first time ill-posed problems have been solved to obtain results of engineering interest; see, for example, Ref. 15, pp. 448-472.

Fictitious Gas

As mentioned above, modifications are made to the basic equations to retain their elliptic behavior once the flow has accelerated to sonic speed and a parabolic surface, with the needed initial data, has been generated. The possible modifications are manifold. We limit our discussion to those we have used to obtain the results reported here.

For two-dimensional flows we have used Jameson's[16,17] circle-plane algorithm for the full potential equation. Thus, in the analysis mode, we are solving

$$\{\rho\phi_x\}_x + \{\rho\phi_z\}_z = 0 \tag{1a}$$

with

$$\rho/\rho_\infty = [1 + \frac{\gamma - 1}{2} M_\infty^2(1 - \phi_x^2 - \phi_z^2)]^{1/\gamma-1} \tag{1b}$$

where ϕ is the velocity potential and ρ the density. If we limit our consideration to fictitious gases for which the density is a function of

the square of the velocity, viz., $\rho = \rho(q^2)$, where $q^2 = U^2[\phi_x^2 + \phi_z^2]$, then gas laws of the form

$$\rho/\rho_* = (a_*/q)^P, \quad P < 1, \quad \text{for} \quad q > a_* \tag{1c}$$

will insure elliptic behavior; $P = 1$ gives parabolic behavior and the fictitious and real gases have the same value of $(d\rho/dq)_*$. An alternative choice, and the one we have used most extensively here, is $P = 0$; in this case Equation (1a) becomes Laplace's equation. When the flow would normally be hyperbolic we now solve Equation (1a) with the density-velocity relationship of Equation (1c). A fictitious mass flow, which matches the real mass flux at the sonic surface, is thereby conserved and the velocity field remains irrotational.

For three-dimensional flows we have used the Ballhaus, Bailey, Frick algorithm,[18] as implemented by Mason et al.[19] This is a small perturbation calculation and we adopt the classical conservative formulation here. Thus we solve, in an equivalent form, the system

$$\begin{aligned} -\frac{1}{2}(\gamma + 1)\{u^2\}_x + v_y + w_z &= 0 \\ u_y - v_x &= 0 \\ u_z - w_x &= 0, \end{aligned} \tag{2}$$

where the velocity vector is $\underline{q} = a_*[(1 + u)\underline{i} + v\underline{j} + w\underline{k}]$.

A simple modification (2) is to replace $\{u^2\}_x$ by $-\text{sgn}(u)\{u^2\}_x$ for all u. This system is elliptic except on the sonic surface where

$u = 0$. We may think of the first of Equations (2) as being the consequence of the small perturbation expansion for the density, viz.,

$$\frac{\rho}{\rho_*} - 1 = -u - \frac{\gamma - 1}{2} u^2, \tag{3}$$

whereas the fictitious equation, with u replaced by $-|u|$ for $u > 0$, results from

$$\frac{\rho}{\rho_*} - 1 = -u + \frac{\gamma + 3}{2} u^2; \tag{4}$$

this fictitious gas has the same value for $(d\rho/du)_*$ as the real gas, Equation (3). For three-dimensional design studies, then, we solve Equations (2) with $\{u^2\}_x$ replaced by $-\text{sgn}(u)\{u^2\}_x$; this corresponds to using the densities given by Equations (3) and (4) for $u < 0$ and $u > 0$ respectively.

Calculation of the Hyperbolic Flow Field

As described above, we calculate the flow past a body using the correct equations when the flow is subsonic and a modified, incorrect, set of equations when the flow is supersonic. This calculation serves to define sonic surfaces on which the flow field calculation is switched from the correct equations to the modified ones. Outside this surface, presuming the trailing edge of the wing is subsonic, the solution satisfies the correct equations and the potential at infinity has the correct value for the circulation. If infinity in the physical plane is not mapped to a finite part of the computational plane, then there is, in principle, a need to correct the doublet and nonlinear contributions; in practice, these con-

tributions are small and changes in them negligible. Thus the flow in the elliptic, subsonic, domains is fixed and known, as is the initial data we need on the parabolic surface.

For two-dimensional flows the calculation of the correct hyperbolic behavior is carried out using the method of characteristics. This is done in a hodograph-like working plane in which the characteristics are orthogonal straight lines. If we take $\xi = \theta + \nu$ and $\eta = \theta - \nu$ where θ is the flow deflection angle and ν the Prandtl-Meyer turning angle, then the velocity potential and stream function satisfy

$$\phi_\xi = K(\frac{\xi - \eta}{2})\psi_\xi$$

$$\phi_\eta = -K(\frac{\xi - \eta}{2})\psi_\eta \qquad (5)$$

or equivalently,

$$\frac{d\psi}{d\phi}\Big|_{\xi,\eta=\text{const}} = \pm K^{-1}$$

where the $\pm$ signs refer to ξ,η = const., respectively. Here

$$K(\nu) = K[\nu(q)] = \{|M^2(q) - 1|\}^{1/2}\rho(0)/\rho(q).$$

Values for the velocity potential on the parabolic line, $z = z^*(x)$, and the shape of this line are used along with the usual relations between the spatial coordinates and ϕ and ψ to find ψ on the sonic line. This initial data is then integrated using Equations (5) to determine the locus $\psi(x,z) = 0$ which passes through the intersection of the sonic line with the body surface. The values of z for which $\psi(x,z) = 0$ determine the

new body shape. This shape will have the same slope, and at least theoretically, the same curvature, as the original body at the sonic points. This follows from the observation that flow quantities are not changed at the sonic line; thus the streamwise momentum and normal pressure gradient are unchanged. Consequently the local flow curvature must be the same.

For three-dimensional flows the calculation of the hyperbolic flow field is carried out by a procedure that marches inward from the sonic surface by successive surfaces of constant density (isopycnics) for the full potential equation, or constant axial flow speed, u, for the small perturbation equation. We limit our discussion to the small perturbation equations, as all the results reported here derive from them. Preliminary results using the full potential equation have been obtained by one of the authors (N. J. Yu).

We may either write the Equations (2) in the appropriately scaled form or work with them directly, which we will do here.

We are given an isotach surface $z^*(x,y)$, as shown in Figure 2, on which we know $u = u^* = \text{const.}$, $w = w^*(x,y)$, and $v = v^*(x,y)$. We use the data on this surface, and the surface shape, to calculate

$$z^*_x, \quad z^*_y, \quad w^*_x, \quad w^*_y, \quad v^*_x, \quad v^*_y. \tag{6}$$

Because this data satisfies Equations (2) we can verify that

$$v^*_x = z^*_x w^*_y - z^*_y w^*_x$$

which can be used, if needed, to check the consistency of the initial data. The values given in Equation (6) can now be used to calculate the z

derivatives of u, w, v on $z^*(x,y)$, where $u(x,y,z^*) = \text{const.}$, by using

$$u_z = [z^*_y v^*_x - z^*_x v^*_y - w^*_x]/J$$

$$w_z = [(\gamma + 1)u^* z^*_x w^*_x - z^*_y w^*_y + v^*_y]/J \tag{7}$$

$$v_z = [(\gamma + 1)u^* z^*_x v^*_x - w^*_y - z^*_y v^*_y]/J$$

where J, the Jacobian, $\partial(u,v,w)/\partial(x,y,z)$, is

$$J = (\gamma + 1)u^* z^{*2}_x - z^{*2}_y - 1.$$

When the Jacobian, which is initially negative, vanishes we can no longer compute the z derivatives; this corresponds to the subsequent formation of multi-valued solutions, i.e., limit surfaces. If $J = 0$ occurs before the calculations pro[illegible] a suitable stream surface defined by $w(x,y,0)$, $v(x,y,0)$, then they must be rejected.

With the first of Equations (7) inverted to give $(dz/du)_*$, we take a set increment in u, Δu, to form a new isotach surface $z^*(x,y) + \Delta z^*(x,y)$. This new shape, along with the mean value of u between the two surfaces and the second and third of Equations (7), provides the new values, $w^*(x,y) + \Delta w^*(x,y)$, $v^*(x,y) + \Delta v^*(x,y)$, of w^* and v^* on the next isotach. These values and the shape of the subsequent isotach are then converted to continuous functions by one-dimensional cubic splines in the x and y coordinates. This "onion-peel"-like process is then continued until $z = 0$, unless a limit surface intervenes. In the latter event the solution must be rejected. A more detailed discussion of this procedure is given in Ref. 20.

derivatives of u, w, v on $z^*(x,y)$, where $u(x,y,z^*) = \text{const.}$, by using

$$u_z = [z^*_y v^*_x - z^*_x v^*_y - w^*_x]/J$$

$$w_z = [(\gamma + 1)u^* z^*_x w^*_x - z^*_y w^*_y + v^*_y]/J \qquad (7)$$

$$v_z = [(\gamma + 1)u^* z^*_x v^*_x - w^*_y - z^*_y v^*_y]/J$$

where J, the Jacobian, $\partial(u,v,w)/\partial(x,y,z)$, is

$$J = (\gamma + 1)u^* z^{*2}_x - z^{*2}_y - 1.$$

When the Jacobian, which is initially negative, vanishes we can no longer compute the z derivatives; this corresponds to the subsequent formation of multi-valued solutions, i.e., limit surfaces. If $J = 0$ occurs before the calculations produce a suitable stream surface defined by $w(x,y,0)$, $v(x,y,0)$, then they must be rejected.

With the first of Equations (7) inverted to give $(dz/du)_*$, we take a set increment in u, Δu, to form a new isotach surface $z^*(x,y) + \Delta z^*(x,y)$. This new shape, along with the mean value of u between the two surfaces and the second and third of Equations (7), provides the new values, $w^*(x,y) + \Delta w^*(x,y)$, $v^*(x,y) + \Delta v^*(x,y)$, of w^* and v^* on the next isotach. These values and the shape of the subsequent isotach are then converted to continuous functions by one-dimensional cubic splines in the x and y coordinates. This "onion-peel"-like process is then continued until $z = 0$, unless a limit surface intervenes. In the latter event the solution must be rejected. A more detailed discussion of this procedure is given in Ref. 20.

TWO-DIMENSIONAL RESULTS

We have explored, rather extensively, some of the modifications that can be made to an existing airfoil, namely an NACA 64A410 airfoil, to obtain shock-free flow. We will call this the baseline airfoil, as the airfoil shapes we generate are identical with this airfoil over that portion wetted by subsonic flow; we need only modify the airfoil over a limited portion of its upper surface to obtain shock-free flows. Further, this modification is not unique for fixed flight conditions; rather, if one such shape exists, there will be an infinite family of modifications of the baseline airfoil that will produce shock-free flow.

With a baseline airfoil selected, here mainly for illustrative purposes, we then pick a set of flight conditions for which we wish to find a modification of the airfoil shape that will result in shock-free flow. We choose $M_\infty = 0.72$ and α, the angle of attack, 0.4 DEG. At these conditions inviscid flow calculations for the NACA 64A410 baseline airfoil give a C_L of 0.78 and a C_D of 0.0064. The design procedure discussed above results in an airfoil that is 9.3% thick and has a lift coefficient of 0.703. The original and the design pressure coefficient, sonic lines, and body shapes are compared in Figure 3a; these results, and all other "analysis" results were computed using the numerical algorithm of Ref. 16. Figure 3b compares the pressure coefficients and sonic lines determined by the design procedure with those computed for the design airfoil shape.

With this shock-free design established at $M = 0.72$ and with $C_L = 0.70$, we now wish to determine the families of shapes that provide shock-free flow for fixed lift coefficient as the Mach number varies, and fixed Mach number as the lift coefficient varies. This we have done with $P = 0$,

that is, with a constant density fictitious gas (at the critical value). We have then explored other shapes that will produce the same lift coefficient, 0.70, at a fixed Mach number, for three different Mach numbers, by taking P to be -0.5, 0.5, and 1.0. Also, for P = 0 we have determined the maximum Mach number for which the design procedure will produce a shock-free airfoil, as a function of lift coefficient. This Mach number is nearly a linear function of lift coefficient at larger lift coefficients. The slope of this variation is consistent with that given by Boerstoel.[21] Preliminary studies also indicate that for a fixed lift coefficient of 0.6–0.7, an 0.1% increase in the maximum Mach number requires about an 0.2% reduction in the thickness for shock-free flow, when the nominal thickness is about 10%. This result is less optimistic than the envelope of the hodograph designs given by Boerstoel,[21] who found that only an 0.1% reduction was required. In our study the generic family of the airfoil is invariant; we have not yet examined the modifications required when the baseline airfoil is near the envelope of hodograph designs. Positive values of P provide less airfoil thickness reduction, as the fictitious and real gas densities are more nearly the same. The range of our airfoil studies is depicted in Figure 4, with shock-free airfoils being determined for the points indicated. Also shown in Figure 4 is the maximum Mach number for which a design was found as a function of lift coefficient for P = 0.

The accuracy of the design procedure was studied at a number of design points by comparing the design's pressure distribution and sonic line shape with those obtained using the unmodified numerical algorithm to analyze the design airfoil shape. Typical results are shown in Figure 5. The sonic line shape and initial data on the sonic line are determined in the circle-

plane; they then are mapped back to the physical plane. The method of characteristics in the hodograph variables is used to compute the design pressure coefficient corresponding to the calculated airfoil surface shape. The agreement, as shown, is excellent. For designs that approach the Mach number at which a limit line first penetrates the surface special care must be taken with the analysis code in order to obtain a converged solution. These designs have very rapid expansions immediately following the sonic line. Indeed, as Boerstoel[21] has noted, the analysis code used with an optimization scheme will not produce designs of this character.

The shock-free airfoil shapes that are obtained for fixed C_L and P, fixed M_∞ and P, and fixed M_∞ and C_L at various P's, are shown in Figures 6-8. One can overlay the results for fixed C_L and find quite similar airfoil shapes that are shock-free over a range of Mach numbers. Because modifications to the baseline airfoil are required only over a limited portion of the upper surface, and a family of specified changes in the airfoil curvature is known for each set of flight conditions, a closely related family of shock-free airfoil shapes can be generated. Thus the minor modifications, to a limited portion of a wing surface, needed to produce shock-free flow over a practical range of flight conditions can easily be determined.

THREE-DIMENSIONAL RESULTS

Our first design results using the method described above were for two-dimensional, small perturbation flow past a parabolic arc airfoil. Consequently, we initiated our three-dimensional studies with a rectangular, unswept wing with an aspect ratio of six and a parabolic arc airfoil. We utilized the small perturbation approximation, Equations (2), and a parabolic

thickness distribution; the airfoil was taken to be 6% thick at the center plane. The flow was calculated using the algorithm of Ref. 19, modified to return the equations to elliptic behavior as described earlier. The initial data on the embedded sonic surface was then used to compute the correct flow in the supersonic domain using the "onion peel" algorithm of Ref. 20. This defines new wing surface slopes. The flow past this shock-free design was then analyzed, using the unmodified numerical algorithm. Figure 9 compares the pressure distributions on the original and design wing, at various lateral positions, for $M_\infty = 0.87$. Also shown are the cross sections of the sonic surface at the same lateral stations. The only essential differences in the pressure occur in the supersonic domain, which is consistent with the design process. The modifications made to the wing slope, shown in Figure 10 for several lateral stations, have eliminated the shock wave.

A subsequent, more realistic, calculation was made for the planform sketched in Figure 11. The wing section chosen was an NACA 64A410 profile at the center section and an elliptic thickness distribution. The leading edge sweep was taken to be 30 DEG, the trailing edge 15 DEG and the span to chord ratio five. The sonic surface is also depicted in Figure 11. Figure 12 compares the pressure coefficients on the upper surface of the original wing and the wing designed to be shock free. While the reduction in drag for this wing is small compared to the induced drag, it is clear that the wing modifications have essentially eliminated the shock waves, and, consequently, the wave drag. More importantly, shock wave induced boundary layer separation is avoided.

We pause at this point to stress that the above comparison is obtained by computing the flow past the original wing and the design wing, using the same numerical algorithm. The process that leads to the new wing shape

also provides the pressure on the wing. Because this pressure, and the new design shape, result from a problem that is presumably ill posed, the results were considered suspect until verified by the original numerical algorithm. Our experience with the calculation of the three-dimensional supersonic flow field is limited. But this limited experience seems to confirm that reducing the isotach or lateral mesh size to small values gives results that are indicative of an instability. At this juncture we can only say that results of engineering interest are obtained in three-dimensional flows, no doubt because the flows of interest are frequently those whose behavior is generally smooth and locally analytic.

CONCLUSION

A novel and simple procedure for determining modifications that will make a baseline configuration shock-free for supercritical flight conditions has been delineated. For two-dimensional, inviscid flows, shock-free designs are obtained in seconds on a CYBER 175. Families of airfoils that are shock-free at fixed, as well as varying, flight conditions are found. The same procedure has been applied to three-dimensional wings, resulting in wing modifications that make the wings shock-free when the flow is analyzed with the numerical algorithm that was modified to become a design tool. It can also be applied to the design of shock-free cascades. A unique feature of the procedure is that any code that is effective in computing the flow field may be modified, in various ways, to be a design algorithm if it is coupled with a method for calculating the solution in the supersonic domains for given data on the sonic surfaces. A straightforward marching technique for such computations is described for three-dimensional flows; in two dimensions either the marching procedure or the method of

characteristics may be used for the supersonic domain. The algorithm for the supersonic domain serves to define the modifications needed in the configuration to achieve shock-free flow; these modifications will be limited to that portion of the design shape that are wetted by supersonic flow.

ACKNOWLEDGMENT

This research was carried out by the Computational Mechanics Laboratory of the Department of Aerospace and Mechanical Engineering. The work was supported by AFOSR Grant 76-2954E, NASA Grant NSG-2112, and ONR Contract N00014-76-C-0182. The authors are indebted to the technical monitors for constructive comments and encouragement during the course of this investigation. They also wish to thank Mr. Howard Nebeck for carrying out the calculations for the airfoil studies and Mr. Patrick DeShazo for managing the computer facilities and the development of supporting algorithms.

REFERENCES

1. Morawetz, C. S., "On the Non-existence of Continuous Transonic Flows Past Profiles, I, II, and III," Comm. Pure and Appl. Math. 9, 10, and 11 (1956, 1957, and 1958), 45-68, 107-131, 129-144.

2. Cook, L. P., "A Uniqueness Proof for a Transonic Flow Problem," Indiana Univ. Math. J. 27 (Jan.-Feb. 1977), 51-72.

3. Whitcomb, R. T. and Clark, L. R., "An Airfoil Shape for Efficient Flight at Supercritical Mach Numbers," NASA TM X-1109 (Confidential Report), July 1965.

4. Pearcey, H. H., "The Aerodynamic Design of Section Shapes for Swept Wings," Advan. Aero. Sci. 3 (1962), 227-322.

5. Garabedian, P. R. and Korn, D. G., "Numerical Design of Transonic Airfoils," Numerical Solution to Partial Differential Equations, Vol. II, Academic Press, New York, 1978, 253-271.

6. Nieuwland, G. Y., "Transonic Potential Flow Around a Family of Quasi-elliptical Airfoil Sections," National Lucht-en Ruimtevaart Laboratorium Report TR-T 172, Amsterdam, The Netherlands, 1967.

7. Boerstoel, J. W., "Design and Analysis of a Hodograph Method for the Calculation of Supercritical Shock-free Airfoils," Nationaal Lucht-en Ruimtevaart Laboratorium Report TR 77046 U, Amsterdam, The Netherlands, 1977; also Boerstoel, J. W. and Huizing, G. H., "Transonic Shock-free Aerofoil Design by an Analytic Hodograph Method," AIAA Paper 74-539, Palo Alto, California, June 1974.

8. Sobieczky, H., "Entwurf überkritischer Profile mit Hilfe der rheoelektrischen Analogie," Deutsche Forschungs-und Versuchsanstalt für Luft-und Raumfahrt Report DLR-FB 75-43, Göttingen, West Germany, 1975.

9. Hicks, R. M. and Vanderplaats, G. N., "Application of Numerical Optimization to the Design of Supercritical Airfoils Without Drag-Creep," Soc. Automotive Engineers, Business Aircraft Meeting Paper No. 770440.

10. Hicks, R. and Henne, P. A., "Wing Design by Numerical Optimization," AIAA Aircraft Systems and Technology Meeting, Seattle, Washington, Aug. 1977, AIAA Paper No. 77-1247.

11. Proceedings ATAR Conference, Advanced Technology Airfoil Research, NASA Langley Research Center, March 1978.

12. Sobieczky, H., "Die Berechnung lokaler Räumlicher Überschallfelder," lecture at Gesellschaft für angewandte Mathematik und Mechanik, Copenhagen, May-June 1977, ZAMM 58T (1978), 215-216.

13. Sobieczky, H., "Transformation Methods for Three-dimensional Compressible Flow," Deutsche Forschungs-und Versuchsanstalt für Luft-und Raumfahrt Report, Göttingen, West Germany, in preparation.

14. Sobieczky, H. and Seebass, A. R., "Adaptive Airfoils and Wings for Shock-free Supercritical Flight," Invention Disclosure, University of Arizona, Tucson, Arizona, May 1978.

15. Hayes, W. D. and Probstein, R. F., Hypersonic Flow Theory, Vol. I, Inviscid Flows, Academic Press, New York, 1966.

16. Jameson, A., "Iterative Solution of Transonic Flows Over Airfoils and Wings," Comm. Pure and Appl. Math. 27 (1974), 283-309.

17. Bauer, F., Garabedian, P., Korn, D., and Jameson, A., "Supercritical Wing Sections," Lecture Notes in Economics and Mathematical Systems, M. Beckmann and H. P. Kunzi (Eds.), Vol. 108, Springer-Verlag, Berlin, Heidelberg, New York, 1975.

18. Ballhaus, W. F., Bailey, F. R., and Frick, J., "Improved Computational Treatment of Transonic Flow about Swept Wings," Advances in Engineering Sciences, NASA CP-2001, 1976.

19. Mason, W. H., Mackenzie, D., Stern, M., Ballhaus, W. F., and Frick, J., "An Automated Procedure for Computing the Three-dimensional Transonic Flow over Wing-body Combinations, Including Viscous Effects," Vols. I and II, Air Force Flight Dynamic Laboratory Report AFFDL-TR-77, Wright-Patterson Air Force Base, Ohio, Feb. 1978.

20. Sobieczky, H., "A Computational Algorithm for Embedded Supersonic Flow Domains," University of Arizona Engineering Experiment Station Report, Tucson, Arizona, July 1978.

21. Boerstoel, J. W., "Review of the Application of Hodograph Theory to Transonic Airfoil Design and Theoretical and Experimental Analysis of Shock-free Airfoils," Symposium Transsonicum II, K. Oswatitsch and D. Rues (Eds.), Springer-Verlag, Berlin, Heidelberg, New York, 1976, 109-133.

FIGURES

Figure 1. Sketch of shock-free flow past a lifting wing depicting the sonic surface obtained by introducing fictitious behavior inside this surface that results in elliptic equations. The correct flow in this supersonic domain is subsequently calculated using the initial data on the sonic surface. This calculation provides the wing geometry modifications needed to obtain shock-free flow.

Figure 2. Sketch of two neighboring isotach surfaces used in the calculation of the supersonic domain for Equations (2).

Figure 3. Comparison of the pressure coefficients and sonic lines for the baseline NACA 64A410 and the shock-free airfoil obtained from it by the direct design procedure.

Figure 4. Parameter space explored for the shock-free airfoils that can be obtained when the baseline configuration is an NACA 64A410 airfoil.

Figure 5. Comparison of the pressure coefficient and the sonic line obtained by the design calculation that modifies the airfoil shape with those obtained by computing the flow past the modified airfoil with the numerical algorithm of Ref. 16.

Figure 6. Shock-free airfoil shapes for fixed lift coefficient and varying Mach number. The fictitious gas has a constant density in the supersonic domain. The vertical scale is magnified five times and the baseline airfoil is an NACA 64A410.

Figure 7. Shock-free airfoil shapes for fixed Mach number and varying lift coefficient. The fictitious gas has a constant density in the supersonic domain. The vertical scale is magnified five times and the baseline airfoil is an NACA 64A410.

Figure 8. Shock-free airfoils obtained at the same flight conditions by varying the exponent of Equation (1c) and thus changing the density's dependence on flow speed. The vertical scale is magnified five times and the baseline airfoil is an NACA 64A410.

Figure 9. Sonic surface for the shock-free rectangular wing obtained by modifying a wing with a parabolic arc airfoil section, and the pressure coefficients on the original and modified wing as calculated by the numerical algorithm of Ref. 19. The thickness distribution of the baseline wing is parabolic.

Figure 10. Changes required in the surface slope at various lateral stations to provide shock-free flow over the rectangular wing of Figure 9.

Figure 11. Sonic surface on the shock-free swept wing used that corresponds to the design pressure coefficients shown in Figure 12.

Figure 12. Comparison of the computed pressure coefficient on a swept wing, with an NACA 64A410 center section profile and an elliptic thickness distribution, with the pressure coefficient obtained by computing the flow past the modified wing using the same numerical algorithm. The leading edge sweep is 30 DEG and the trailing edge sweep 15 DEG.

SHOCK - FREE FLOW PAST A LIFTING WING

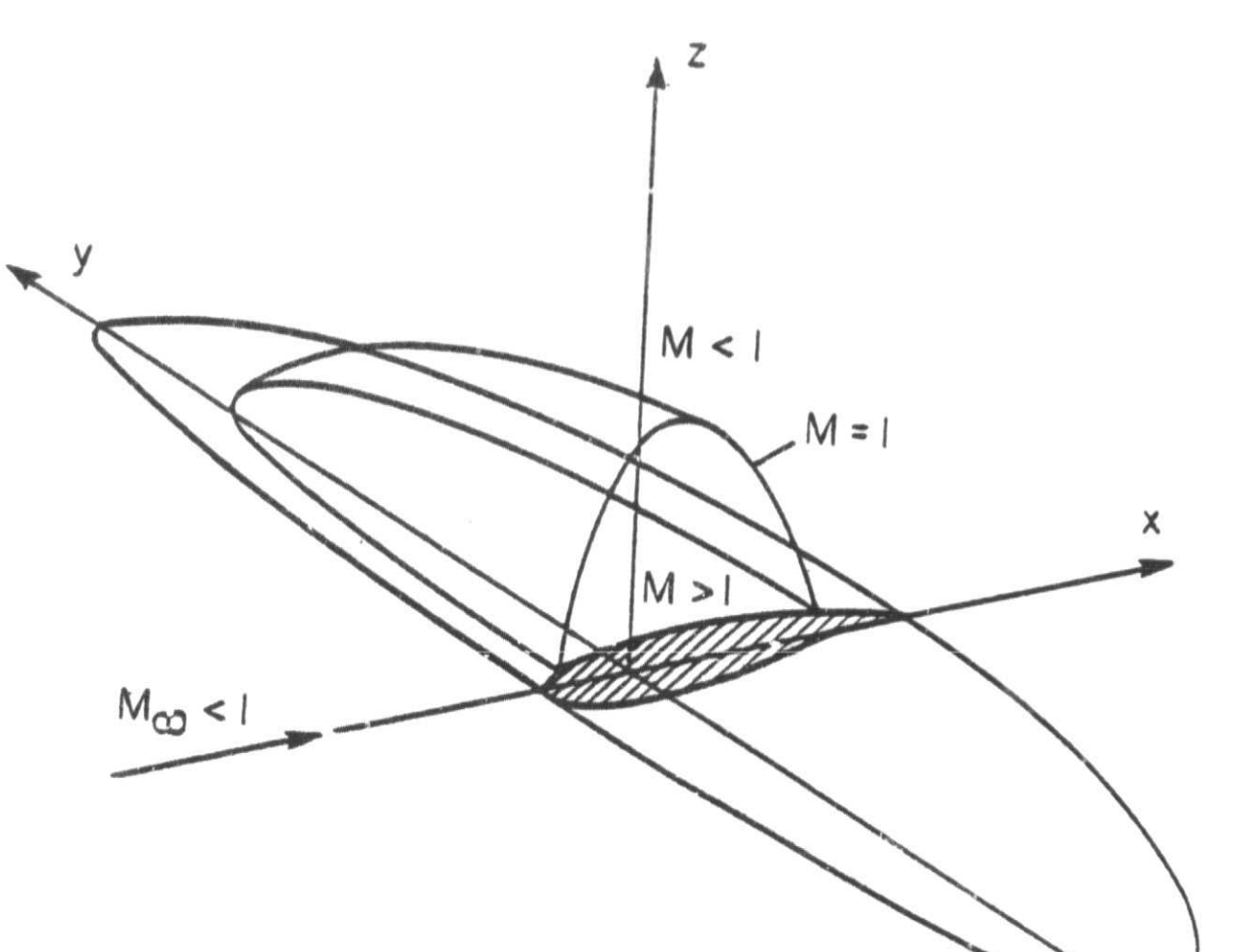

FIGURE 1

ISOTACH SURFACES USED IN
CALCULATING HYPERBOLIC DOMAIN

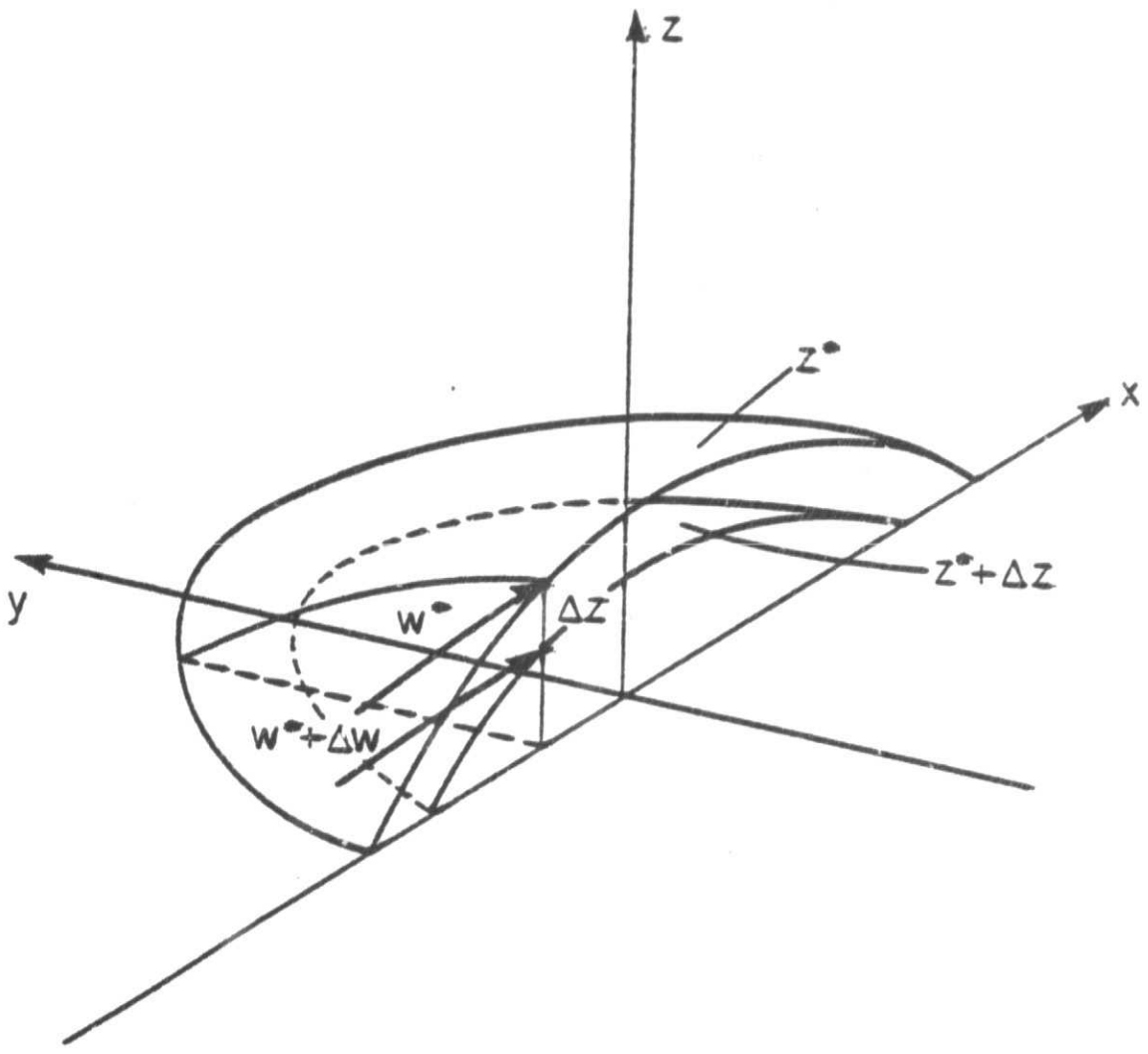

FIGURE 2

COMPARISON OF NUMERICAL ANALYSIS RESULTS FOR ORIGINAL AND SHOCK-FREE AIRFOIL

(BASELINE AIRFOIL: NACA 64A410)

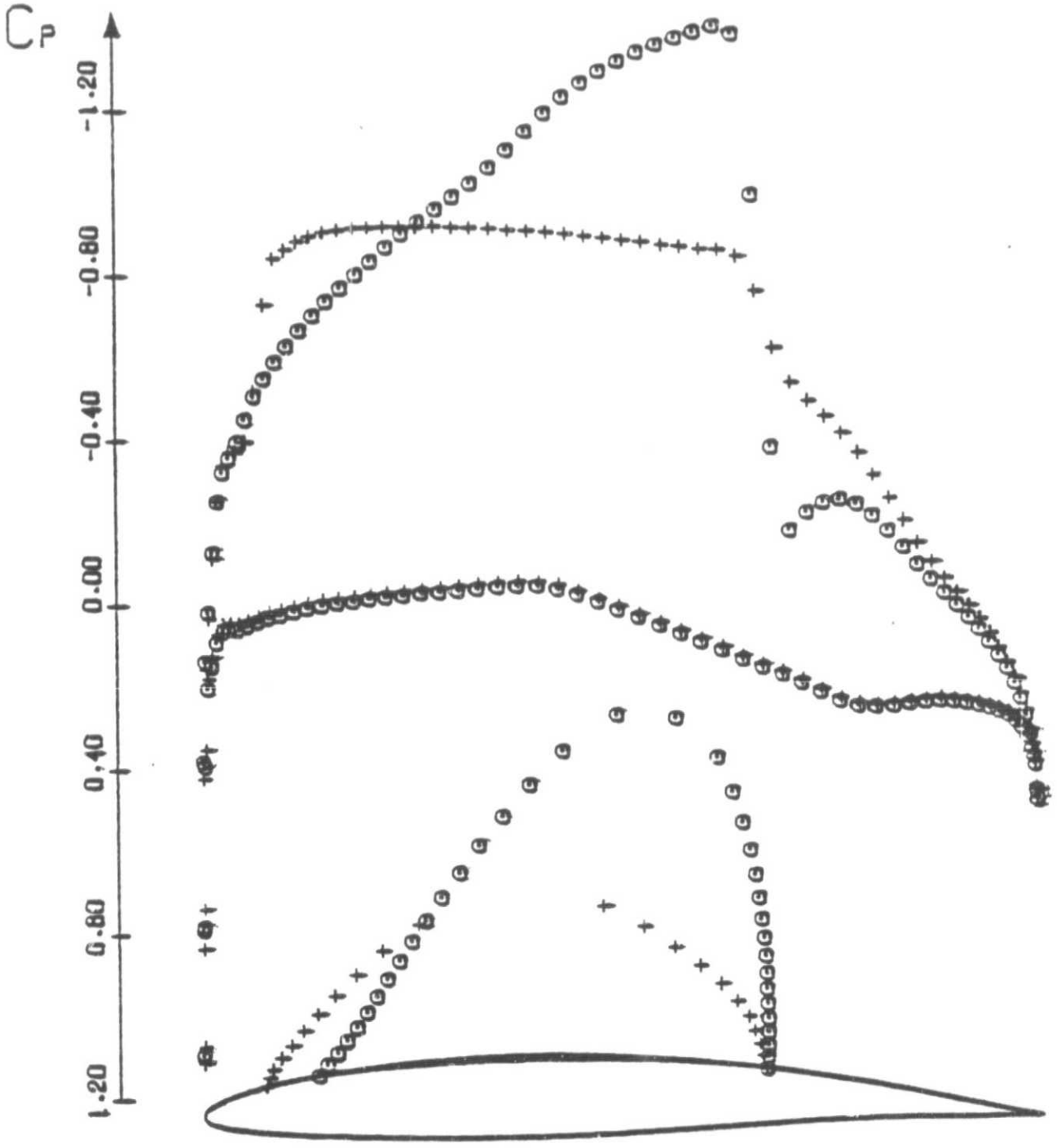

MACH = .720 ALPHA = 0.40

	DESIGN (+)	ORIGINAL (⊙)
CL	0.7029	0.7799
CD	0.0000	0.0064
CM	-.1397	-.1601

FIGURE 3

FLOW CONDITIONS AND FICTITIOUS GAS LAWS STUDIED
Baseline airfoil NACA 64A410

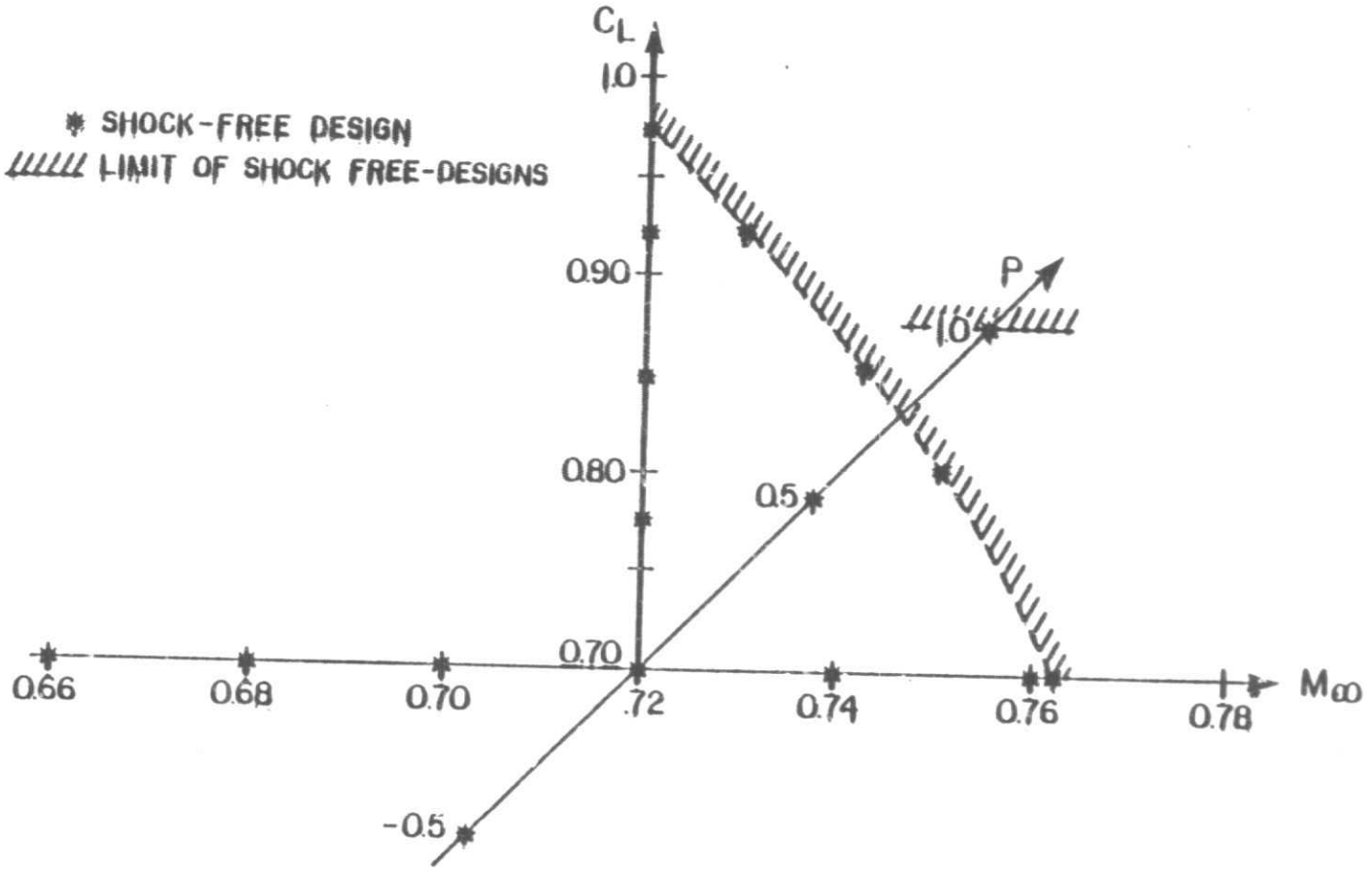

FIGURE 4

COMPARISON OF DESIGN AND ANALYSIS RESULTS

(BASELINE AIRFOIL: NACA 64A410)

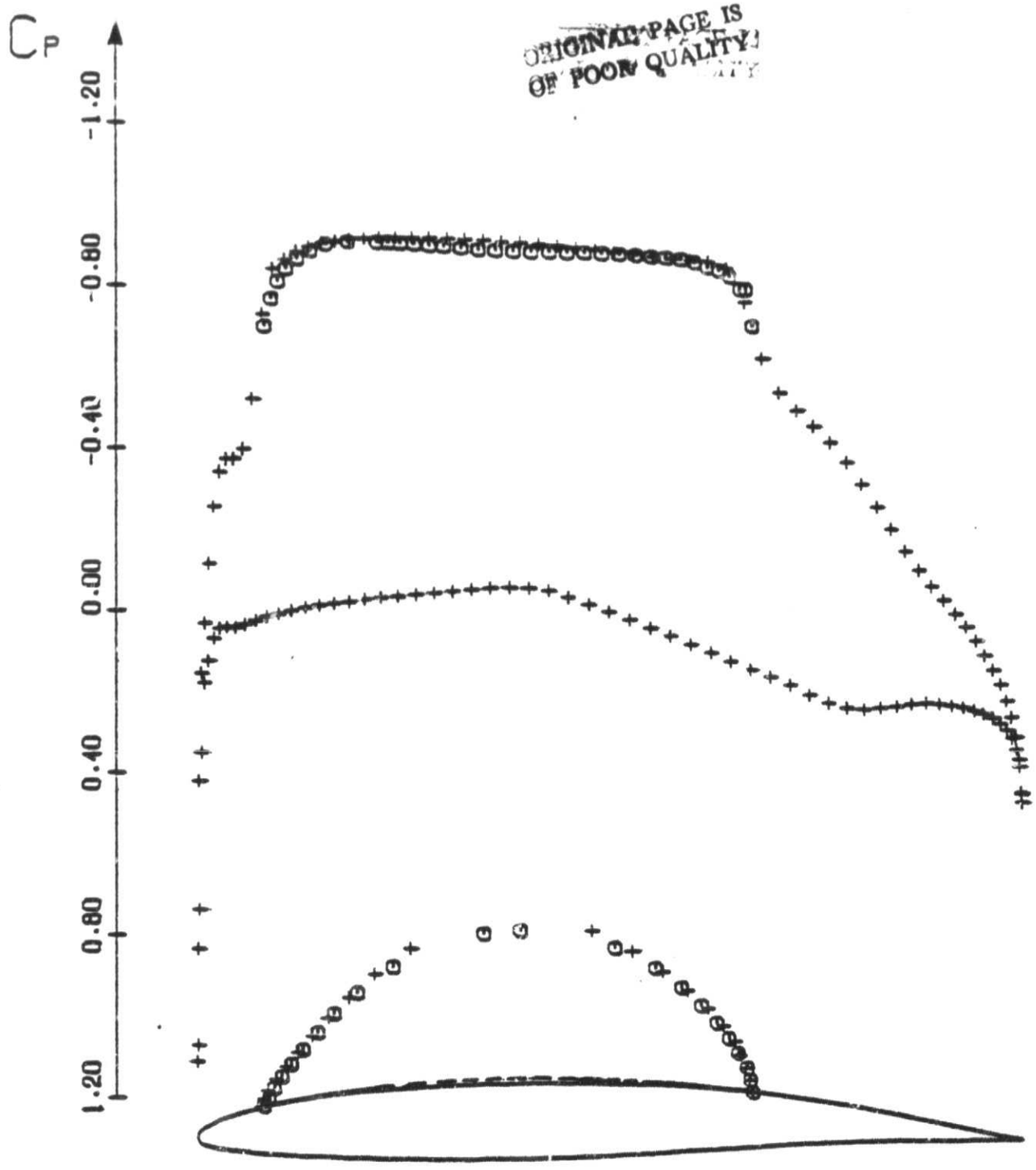

MACH = .720 ALPHA = 0.40

	DESIGN (⊙)	ANALYSIS (+)
CL	0.7012	0.7029
CD	0.0001	0.0000
CM	-.1395	-.1397

FIGURE 5

SHOCK-FREE AIRFOIL SHAPES

$C_L = 0.70, \quad P = 0.$

(BASELINE AIRFOIL: NACA 64A410)

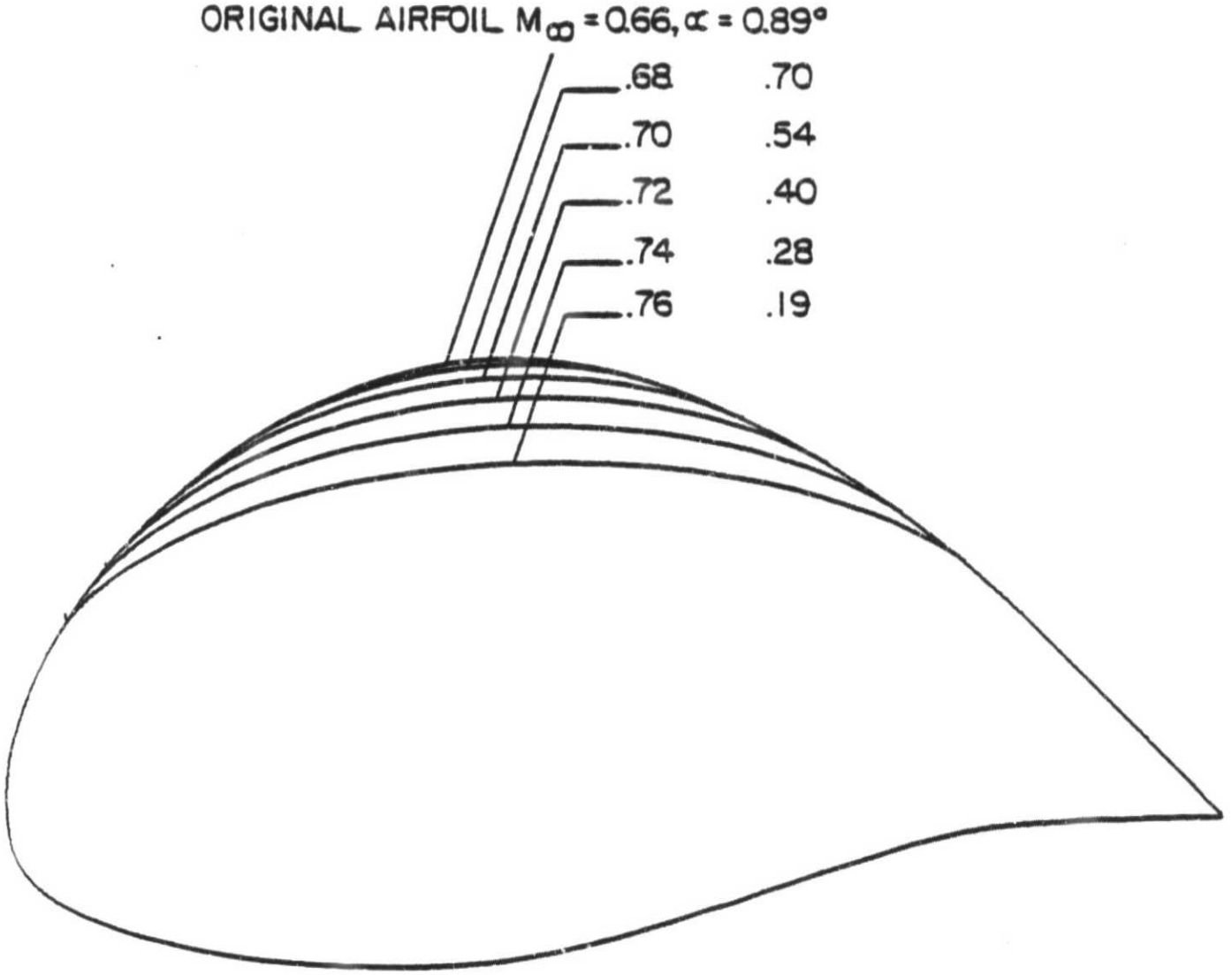

Y SCALE = 5*(X SCALE)

FIGURE 6

SHOCK-FREE AIRFOIL SHAPES

$M_\infty = 0.72, \quad P = 0.$

(BASELINE AIRFOIL: NACA 64A410)

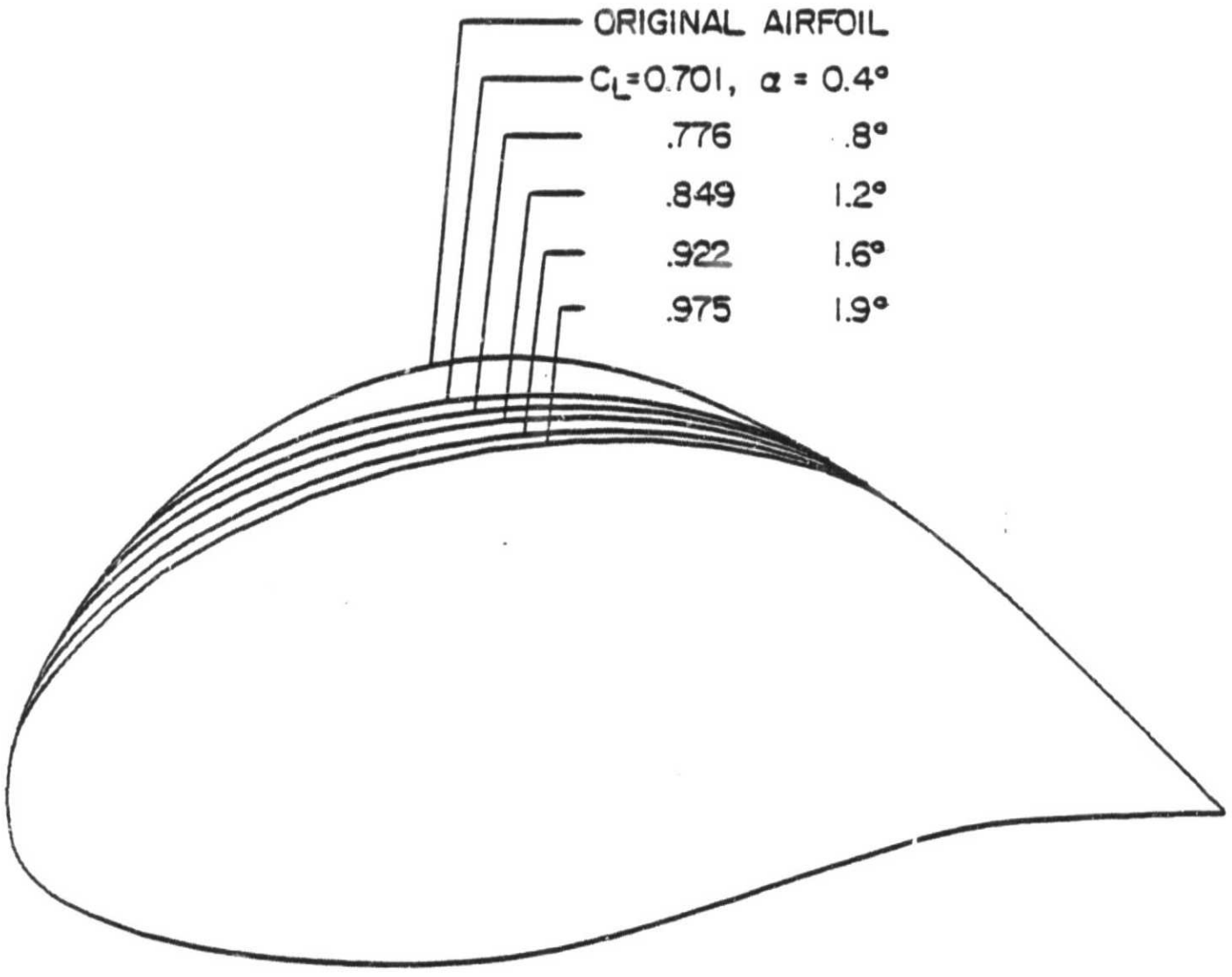

Y SCALE = 5*(X SCALE)

FIGURE 7

SHOCK-FREE AIRFOIL SHAPES

$M_\infty = 0.72, \quad C_L = 0.70$

(BASELINE AIRFOIL: NACA 64A410)

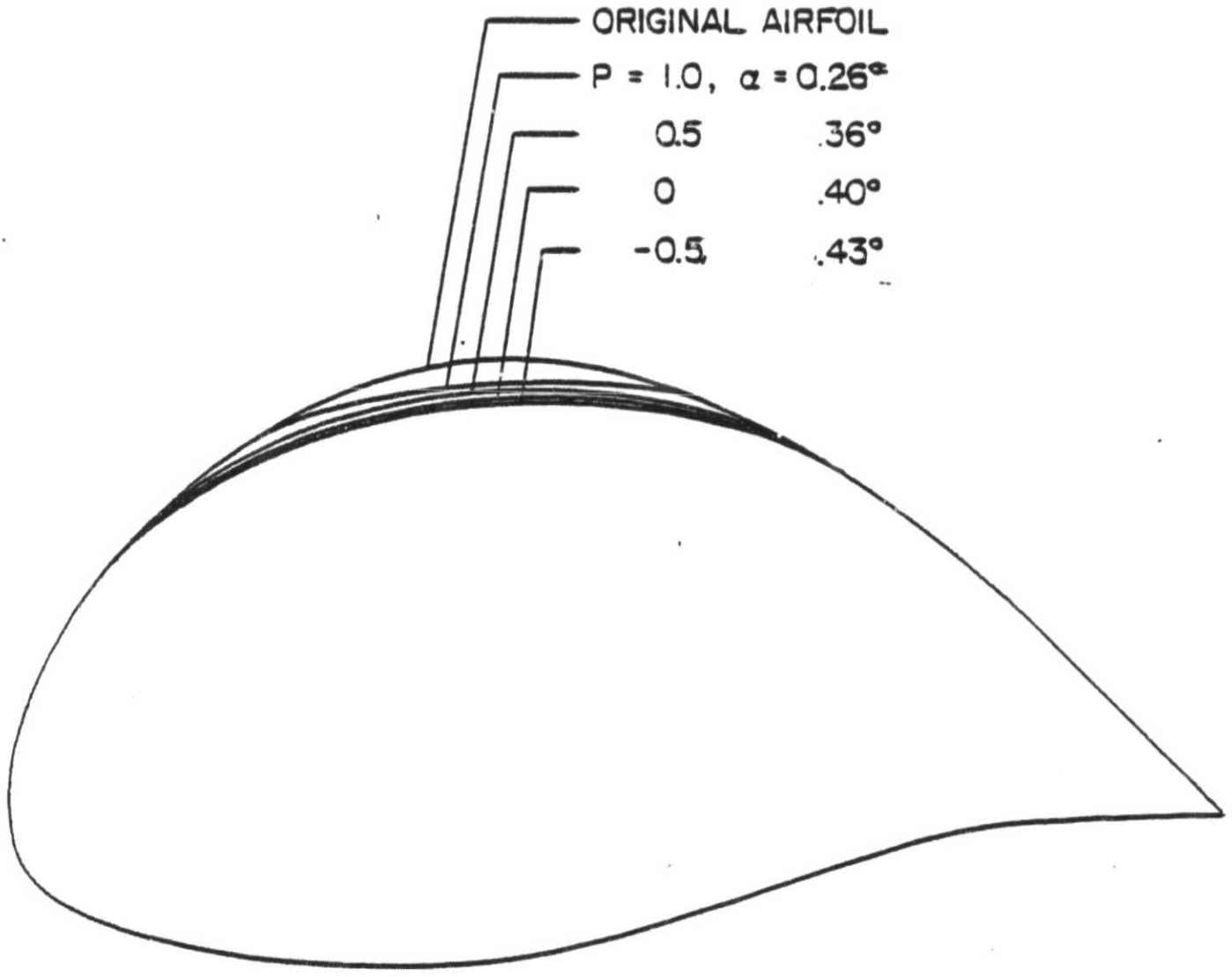

Y SCALE = 5*(X SCALE)

FIGURE 8

PRESSURE COEFFICIENTS AND SONIC SURFACE ON A RECTANGULAR WING
ORIGINAL WING IS 6% THICK PARABOLIC ARC IN CENTER PLANE
THICKNESS DISTRIBUTION IS PARABOLIC
$M_\infty = 0.87$

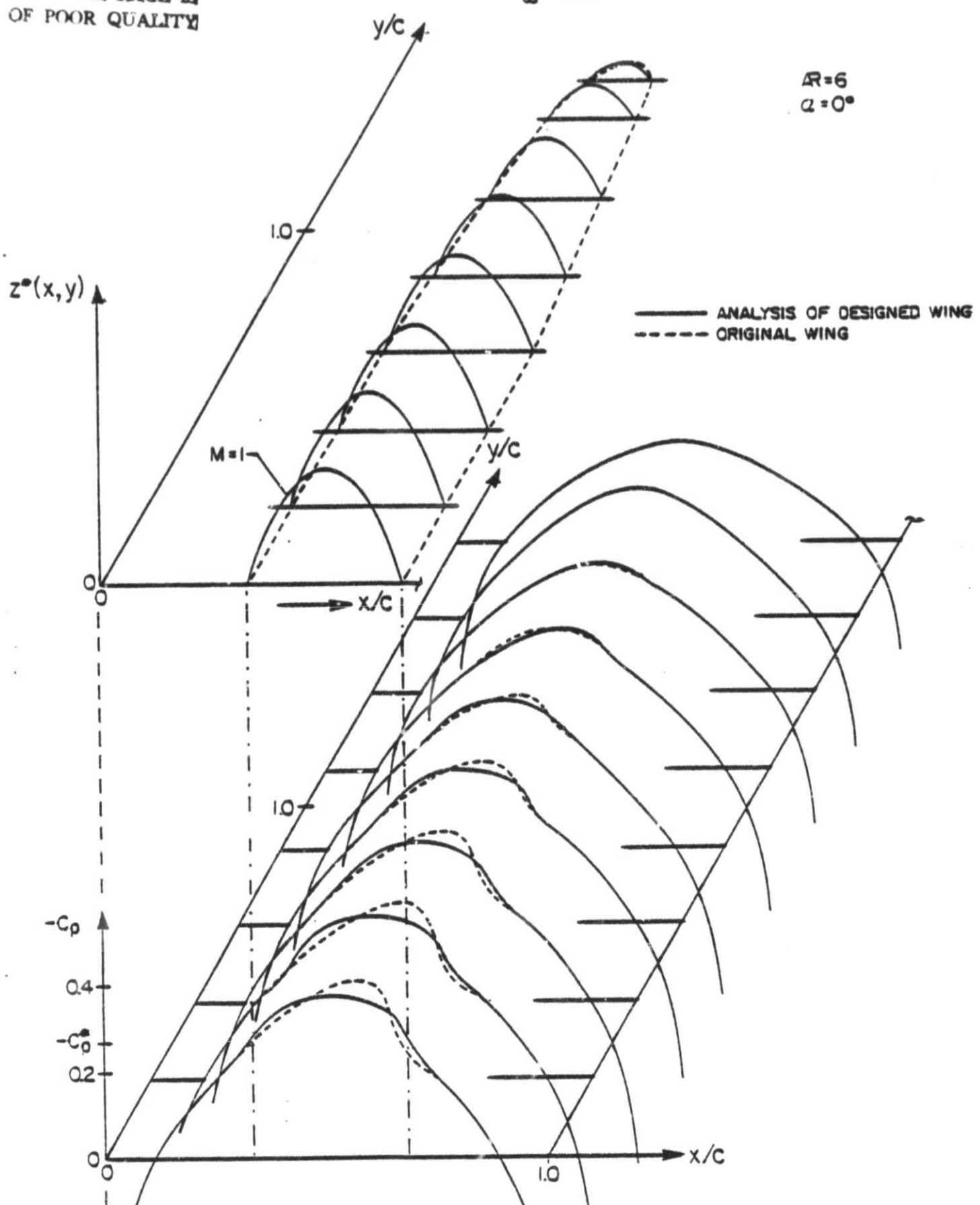

FIGURE 9

CHANGE IN SURFACE SLOPE REQUIRED FOR SHOCK-FREE DESIGN

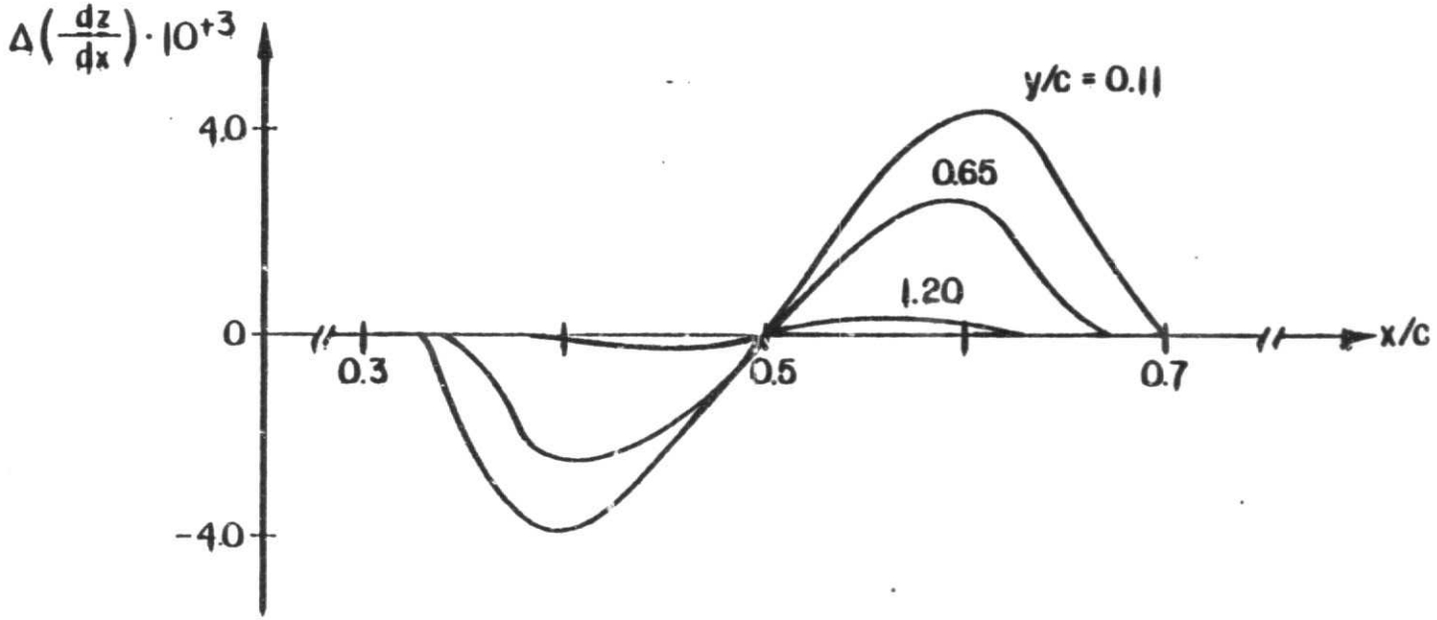

FIGURE 10

SONIC SURFACE ON A SWEPT WING
ORIGINAL WING IS NACA 64A410 SECTION IN CENTER PLANE
THICKNESS DISTRIBUTION IS ELLIPTICAL

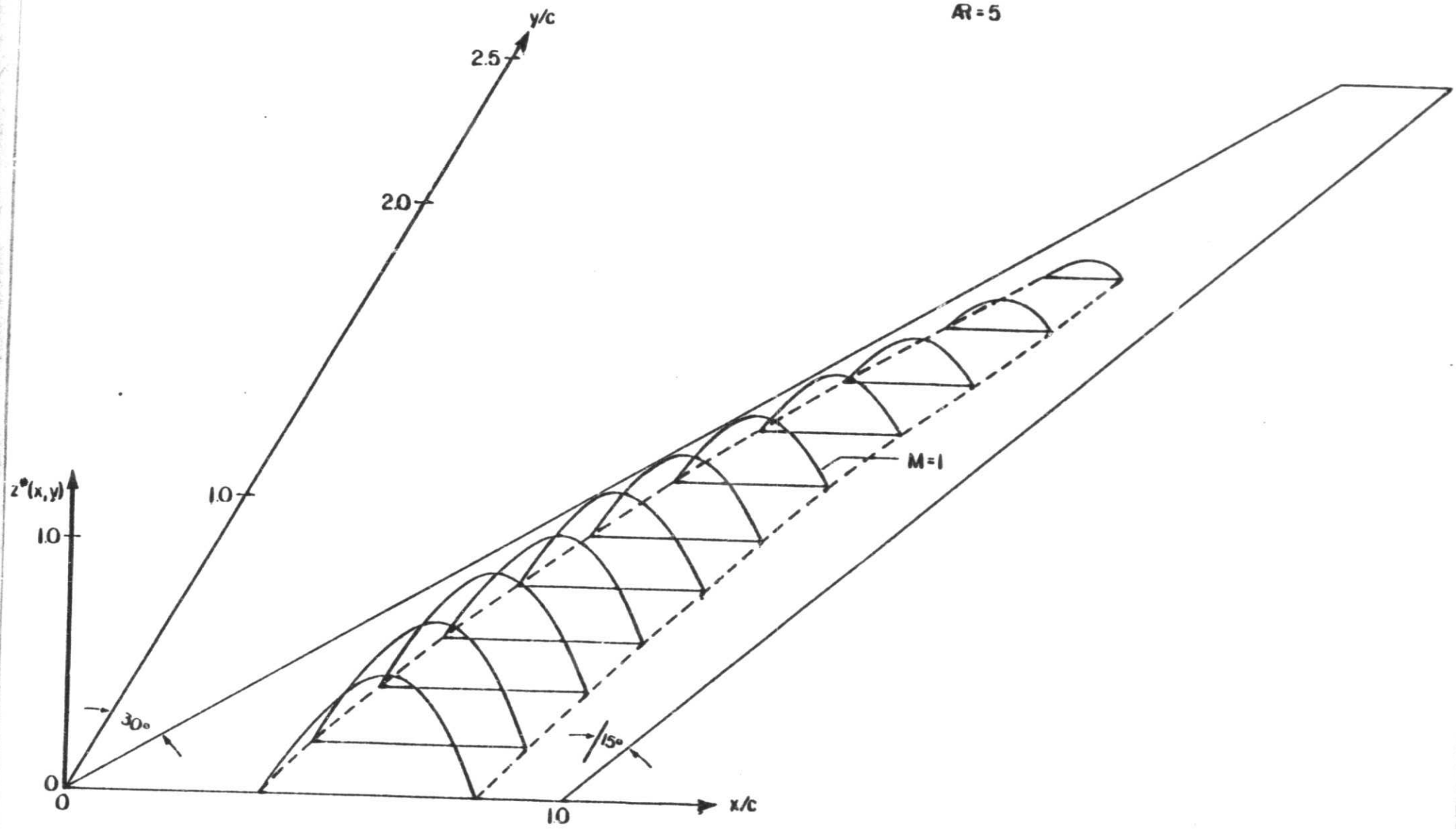

FIGURE 11

PRESSURE COEFFICIENTS ON ORIGINAL AND MODIFIED SWEPT WING
ORIGINAL WING IS NACA 64A410 AIRFOIL IN CENTER PLANE
THICKNESS DISTRIBUTION IS ELLIPTICAL
$M_\infty = 0.80$

AR = 5